Available online at www.sciencedirect.com
SCIENCE DIRECT®
Journal of Sound and Vibration 293 (2006) 112–124
JOURNAL OF SOUND AND VIBRATION
www.elsevier.com/locate/jsvi

# Railway vehicle/track interaction analysis using a modal substructuring approach

L. Baeza[a,*], A. Roda[a], J.C.O. Nielsen[b]

[a]*Departamento de Ingeniería Mecánica y de Materiales, Universidad Politécnica de Valencia, Camino de Vera s/n, 46022 Valencia, Spain*
[b]*Department of Applied Mechanics/CHARMEC Chalmers University of Technology, SE-412 96 Göteborg, Sweden*

Received 28 September 2004; received in revised form 4 July 2005; accepted 22 September 2005
Available online 8 November 2005

**Abstract**

A method for simulation of the dynamic interaction between vehicle and railway track is proposed. The model has been designed to take into account the complexity of wheel–rail contact, railpad and ballast, with low computational requirements. A modal description of the rails and the sleepers is presented, imposing the coupling between these elements and the vehicle by means of the associated interaction forces. This provides a model with a reduced number of coordinates and therefore a low computational cost is achieved. It is shown that this model also enables to incorporate the associated nonlinear characteristics between the different elements by means of a simple formulation.


## 1. Introduction

Railways are experiencing a significant set of problems associated with dynamic interaction of the vehicle–track system. These problems mainly stem from existing wheel and track defects and they affect acoustic emissions, track maintenance and the reliability of the vehicle's rolling elements.

In order to study these problems, models have been developed which make it possible to simulate the dynamic response of vehicle–track interaction. Only simple models, which consider the rail as a beam resting on an elastic foundation, have an analytical solution. This simplicity is lost when the rail is considered as having discrete supports and when nonlinearities are associated with the properties of ballast, railpads and wheel–rail contact. Several authors have proposed methodologies for studying vehicle–track dynamics (see the surveys in Refs. [1,2]). Perhaps, the most commonly studied problems concern the formation of irregular wear (corrugation) on wheels and rails, and the dynamic response to wheelflat impact (part of the wheel tread is worn off due to unintentional sliding as caused by locked brakes or by low wheel–rail friction). In these two cases the frequency range considered is similar, so the basic dynamic model characteristics are the same for both problems.

Of particular note among models with an analytical solution are the works of Grassie et al. [3], Patil [4] and Duffy [5], where the track is considered as a beam on an elastic foundation. In Ref. [3], Grassie highlights the

*Corresponding author. Tel.: +34 963877621; fax: +34 963877629.
*E-mail address:* lbaeza@mcm.upv.es (L. Baeza).

0022-460X/$ - see front matter © 2005 Elsevier Ltd. All rights reserved.
doi:10.1016/j.jsv.2005.09.006

need to improve the models by introducing the track on discrete supports. This improvement makes it possible to increase the valid frequency range of the models by considering certain types of characteristic vibration modes of the track, as for example the pinned–pinned resonance [1]. Some models [3] are based on calculating a track frequency response function (FRF), although these models cannot consider local nonlinearities in for example mechanical properties of ballast and railpad. Models which incorporate nonlinearities in track properties and wheel–rail contact have been developed in Refs. [6–9]. The dynamic interaction is solved by time integration of the equations of motion obtained from a finite element (FE) model incorporating forces as nonlinear functions of displacement and velocity. As indicated in Ref. [8], the main disadvantage in using these models is computational cost, because a very large number of coordinates needs to be considered.

By considering the dynamic model on the basis of a set of coordinates which defines the phase space associated to the track in the studied frequency range, it is possible to reduce problem size and consequently computational cost. Thus, in Ref. [10], Wu and Thompson proposed a set of coordinates for establishing the phase space associated to the track FRF. This technique makes it possible to model wheel–rail interaction realistically, providing the transient responses of track and vehicle at low computational cost. However, there are certain limitations, since the track model is linear and only a small number of vibration modes can be considered (corresponding to the number of FRF poles).

To define computationally efficient models, the applications of different dynamic substructuring techniques have been proposed. For example, in Ref. [11], a modal description of the wheelset is proposed to model its dynamic behaviour, coupling it to a FE rail model by the corresponding interaction forces.

In this paper, a new method for calculating the dynamic response of the vehicle–track system is developed that can take into account complex models of wheel–rail contact, railpads and ballast at low computational cost. The rails and the sleepers are described by their modal coordinates. Wheel–rail, rail–sleeper and sleeper–ballast interactions are modelled using space coordinates and they are coupled to the modal models of rail and sleeper by means of the corresponding interaction forces. The overall model is described by a reduced number of coordinates. In addition, the most significant nonlinearities of the problem can be included easily.

## 2. Vehicle–track dynamic model

### 2.1. Track modelling

The developed track model is based on a substructuring approach, where a modal description of each isolated rail and sleeper is adopted. Ballast and railpads are considered as connection elements, where the ballast connects sleepers and ground and the railpads connect sleepers and rails.

The dynamic behaviour of the isolated substructures (rails and sleepers) is described by linear beam theory. The sleepers are modelled as Euler beams on a Winkler foundation, where the ballast is the elastic foundation. Therefore, initially, ballast is considered as having linear characteristics. However, it is possible to include nonlinearities as proposed in Ref. [6] by incorporating them as external forces as a function of sleeper displacements. Without losing the generality of the methodology developed here, only vertical train–track dynamics is considered in the present study. This is justified because the present application is dominated by such interaction.

The global coordinate system $xyz$ is defined with the positive $x$-axis parallel to the rail in the direction of vehicle motion. The $y$-axis is transverse to the track and the vertical $z$-axis is positive upwards. Fig. 1 illustrates

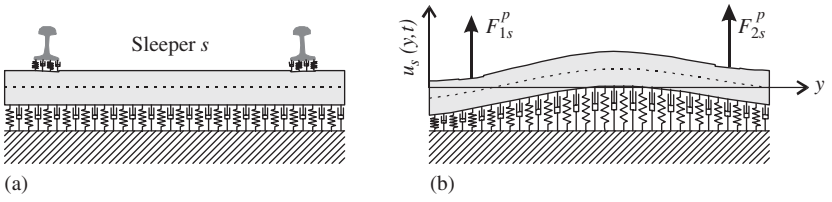


Fig. 1. Model of sleeper.

the sleeper model. Vertical displacements of sleeper $s$ are given by the function $u_s(y,t)$, where $y$ is the coordinate of the studied section. Forces $F^p_{rs}$ exerted by the rails through the railpads are applied on the rail seats in $y = d_r$ (index $r = 1, 2$ corresponds to the right and left rail, respectively).

The mode shape $\psi_n(y)$ of the $n$th non-damped mode is mass-normalised, and $\omega_n$ is the natural angular frequency (mode numbers $n = -1$ and 0 are reserved for modes which do not produce elastic strain in the beam). Modal properties are calculated analytically according to Ref. [12]. Damping is considered through the modal damping rate $\xi_n$ associated to each sleeper mode.

The transformations, which relate physical sleeper displacements to modal coordinates and forces transmitted through the railpads to modal forces, are

$$u_s(y,t) = \sum_{n=-1}^{N_{ms}} \psi_n(y) q^S_{sn}(t), \quad f^S_{sn}(t) = \sum_{r=1}^{2} F^p_{rs} \psi_n(d_r), \tag{1}$$

where $q^S_{sn}(t)$ and $f^S_{sn}(t)$ represent the modal coordinate and the modal force associated to mode $n$ of sleeper $s$, respectively. Modal truncation is performed considering a finite number $N_{ms}$ of sleeper modes.

In the model, the rails are treated as Timoshenko beams. Vertical rail displacement is defined by the variable $v_r(x,t)$, where $x$ is the coordinate which defines the location of the beam section (see Fig. 2). Sleeper $s$ is located in rail section $x = b_s$. Consider a vehicle with $N_{ax}$ wheelsets. The position of each wheelset is $x = c_a + Vt$, where $V$ is the vehicle speed, $c_a$ is the corresponding initial coordinate and subindex $a$ is an integer which numbers the wheelsets. Each rail $r$ is acted upon by a set of forces $F^p_{rs}$ exerted by the sleepers through the railpads, and another set of forces $F^c_{ra}$ transmitted by the wheels through the wheel–rail contacts.

The rail model in this work is also based on a modal description. Let $\lambda_m$ and $\phi_m(x)$ be the $m$th non-damped natural angular frequency and the corresponding mass-normalised vibration mode shape of an isolated rail, respectively (subindex $m$ varies from $-1$ to the number of rail modes $N_{mr}$; reserving mode numbers $m = -1$ and 0 for rigid body modes which do not produce elastic strain in the beam). Considering the rail as a Timoshenko beam with free–free boundary conditions, the corresponding mode shapes and natural frequencies can be determined analytically according to Ref. [13]. Rail damping is accounted for by the modal damping rate $\zeta_m$. In this case, the modal transformations for the rail are

$$v_r(x,t) = \sum_{m=-1}^{N_{mr}} \phi_m(x) q^R_{rm}(t), \quad f^R_{rm}(t) = \sum_{a=1}^{N_{ax}} F^c_{ra} \phi_m(c_a + Vt) - \sum_{s=1}^{N_s} F^p_{rs} \phi_m(b_s), \tag{2}$$

where $q^R_{rm}(t)$ and $f^R_{rm}(t)$ represent the modal coordinate and the modal force associated to mode $m$ of rail $r$, respectively.

### 2.2. Equations of motion of the track

According to the above track model, the receptance $H^S_n$ corresponding to mode $n$ of an isolated sleeper is

$$H^S_n(\sigma) = \frac{q^S_{sn}}{f^S_{sn}} = \frac{1}{\sigma^2 + 2\xi_n\omega_n\sigma + \omega_n^2}, \tag{3}$$

where $\sigma$ represents the Laplace variable. The model of mode $n$ of sleeper $s$, as given by Eq. (3), can be expressed in the time domain by the following set of equations:

$$\dot{q}^S_{sn}(t) = -2\xi_n\omega_n q^S_{sn}(t) + p^S_{sn}(t), \quad \dot{p}^S_{sn}(t) = -\omega_n^2 q^S_{sn}(t) + f^S_{sn}(t), \tag{4}$$

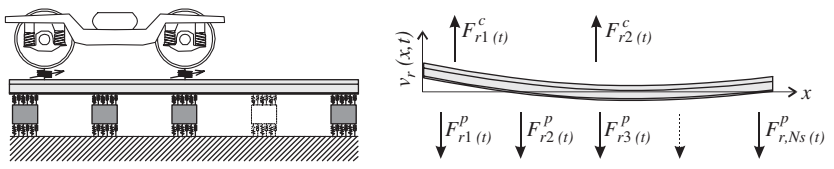


Fig. 2. Model of rail.

where coordinate $p^S_{sn}(t)$ has been introduced along with coordinate $q^S_{sn}(t)$ in order to obtain a base of the phase space for the sleeper dynamics ($s$ varies from 1 to the number of sleepers $N_s$, and $n$ from $-1$ to the number of sleeper modes $N_{ms}$).

Proceeding for each rail in a similar way, the receptance $H^R_m$ is given by

$$H^R_m = \frac{q^R_{rm}}{f^R_{rm}} = \frac{1}{\sigma^2 + 2\zeta_m\lambda_m\sigma + \lambda^2_m}. \tag{5}$$

This leads to the following set of equations of motion:

$$\dot{q}^R_{rm}(t) = -2\zeta_m\lambda_m q^R_{rm}(t) + p^R_{rm}(t), \quad \dot{p}^R_{rm}(t) = -\lambda^2_m q^R_{rm}(t) + f^R_{rm}(t), \tag{6}$$

where coordinate $p^R_{rm}(t)$ has been introduced so that $q^R_{rm}(t)$ and $p^R_{rm}(t)$ form a base of the phase space for the rail dynamics ($r$ varies from 1 to the number of rails $N_r$, and $m$ from $-1$ to the number of rail modes $N_{mr}$).

### 2.3. Vehicle model

The vehicle is modelled as a multibody system where the wheelsets, bogie frames and carbody are considered as rigid bodies joined by means of linear suspensions (see Fig. 3). A set of reference point coordinates, which include centre of mass displacements and rotations of the bodies, is adopted assuming the hypothesis of small displacements. Let $\mathbf{w}(t)$ be the vector containing the vehicle coordinates. For the $a$th wheelset, two independent displacements are studied corresponding to vertical displacement $z_a(t)$ and roll angle $\theta_a(t)$. On each wheelset $a$, forces $F^c_{ra}$ ($r = 1, 2$) from each rail are applied through the wheel–rail contacts.

The equations of motion for the system described above can be written as

$$\mathbf{M}\ddot{\mathbf{w}} + \mathbf{D}\dot{\mathbf{w}} + \mathbf{K}\mathbf{w} = \mathbf{F}_{\text{ext}} + \mathbf{F}_c, \tag{7}$$

where $\mathbf{M}$, $\mathbf{D}$ and $\mathbf{K}$ correspond to the mass, viscous damping and stiffness matrices of the vehicle, and $\mathbf{F}_{\text{ext}}$ is the vector of external forces (such as gravity loads). The vector $\mathbf{F}_c$ contains the forces transmitted through the wheel–rail contacts.

### 2.4. Vertical forces in wheel–rail contact

Wheel–rail interaction is modelled by the contact force $F^c_{ra}$. In general, this force is expressed as a function of the relative displacement between wheel and rail at the contact point, and it depends on the un-deformed wheel–rail geometry and the elastic characteristics of the wheel–rail contact.

Wheel and rail imperfections are accounted for by an irregularity function, which is defined as the vertical wheel displacement assuming no loss of contact and un-deformable wheel and track. A characteristic type of irregularity is associated with the wheelflat. Bearing in mind that a fresh flat is reshaped into a rounded flat shortly after being formed, a cosine function to represent the irregularity function for a rounded flat is often adopted [10,14]. The approach of the centres of the wheel and the rail as a function of angular rotation of the wheel assuming rigid contact for the fresh and the rounded flats are shown in Fig. 4.

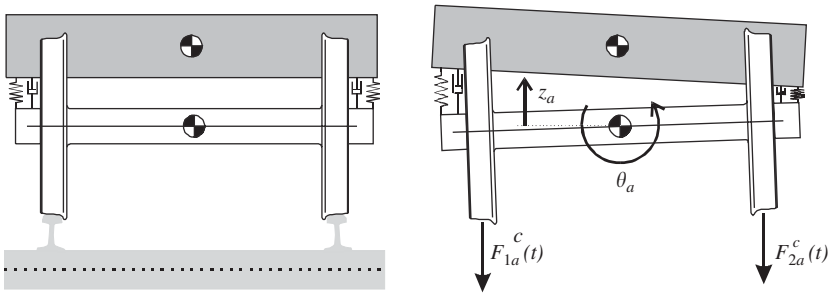


Fig. 3. Model of vehicle.

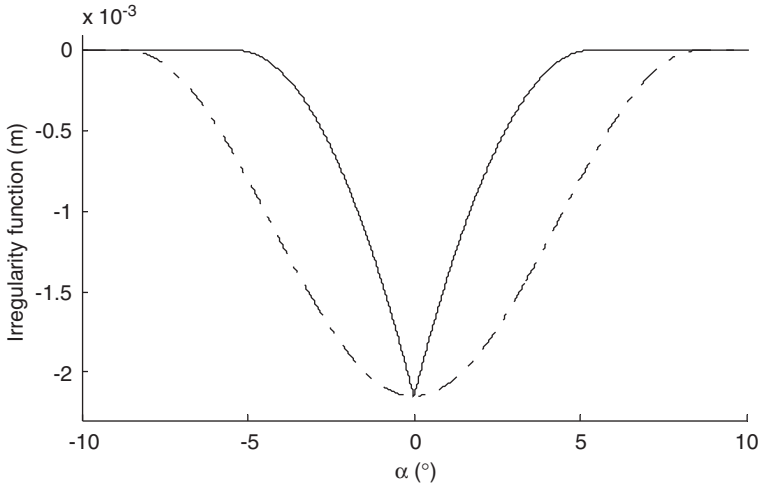


Fig. 4. Irregularity functions for a 92.7 mm fresh flat (solid) and the corresponding 150 mm rounded flat (dash–dotted). $\alpha = 0^\circ$ indicates complete contact with the fresh flat.

To account for the elasticity in the wheel–rail contact, several authors [7,10,14,15] adopt Hertzian models where the force transmitted in the contact is given by the equation

$$F^c = k_H \delta^{1.5}. \tag{8}$$

Here $\delta$ is the approach of the centres of the two elastic bodies in contact, and $k_H$ is a constant which depends on contact geometry and the mechanical characteristics of the materials.

In the case of a fresh flat, the Hertzian model may not be appropriate because the un-deformed wheel surface cannot be described as a paraboloid (according to Hertzian contact conditions in Ref. [16]). However, for typical wheelflat and wheel dimensions, a non-conformal contact hypothesis can be adopted (as defined by Hills and Nowell [17]). This makes it possible to use normal non-Hertzian contact calculation methods such as those developed by Kalker [18].

For example, using Kalker's model in Ref. [18], Fig. 5 shows the approach of the centres for the combined effect of the geometry of the wheelflat and the elastic deformation of the wheel and rail under a static load of 100 kN. The approach is represented as a function of the angular position of the fresh flat relative to the rail. The calculations were performed for a 92.7 mm long wheelflat on a 1000 mm diameter wheel. It is observed that flexibility increases considerably when contact occurs at the fresh flat vertex. However, when there is full wheelflat contact, flexibility decreases very rapidly.

When non-Hertzian contact is considered, a large set of calculations is required and it is not viable to solve this problem simultaneously with the integration of the differential equations of motion. Instead, the non-Hertzian model is precalculated for a set of relative wheelflat positions with respect to the track and for different normal forces in the contact. This makes it possible to interpolate the contact force model in the dynamic simulation. An example of contact model for a fresh flat is shown in Fig. 6, which shows the approach of the wheel and rail centres as a function of both angular rotation of the wheel and static load.

A good fit is obtained for each angular position of the wheel by a function of the type

$$F^c = k\delta^\gamma, \tag{9}$$

where $k$ and $\gamma$ depend on the wheelflat position with respect to the contact. The parameter $\gamma$ is approximately 1.5 (cf. Eq. (8)) except when there is full wheelflat–rail contact, where $\gamma$ is close to 1.

The distribution of normal stresses transmitted between wheel and rail calculated according to the model in Ref. [18] makes it possible to determine the pressure centre and therefore the position of the resultant contact force in relation to the contact patch. The deviation of the application point of the resultant concentrated contact force with respect to the wheel centre position is shown in Fig. 7. This deviation is calculated using

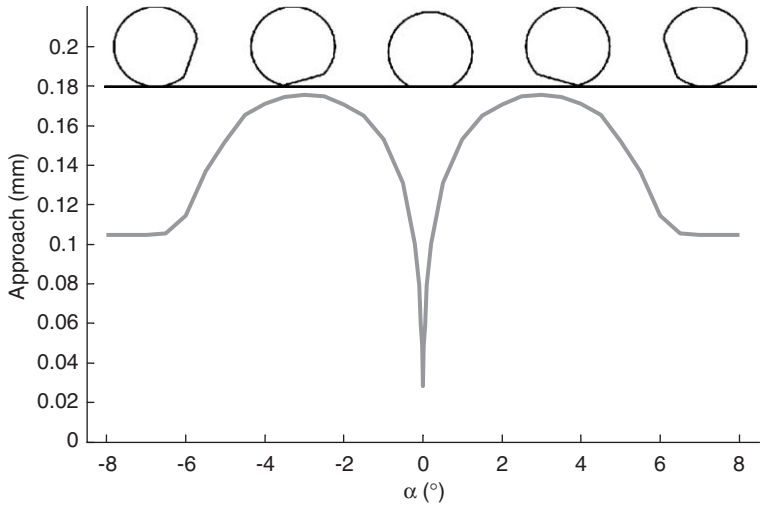


Fig. 5. Approach of centres of the two elastic bodies in contact under a load of 100 kN in relation to angle of wheel rotation. $\alpha = 0^\circ$ indicates complete contact between fresh flat and rail. The sketches of the wheel show the position of the flat with respect to the wheel–rail contact.

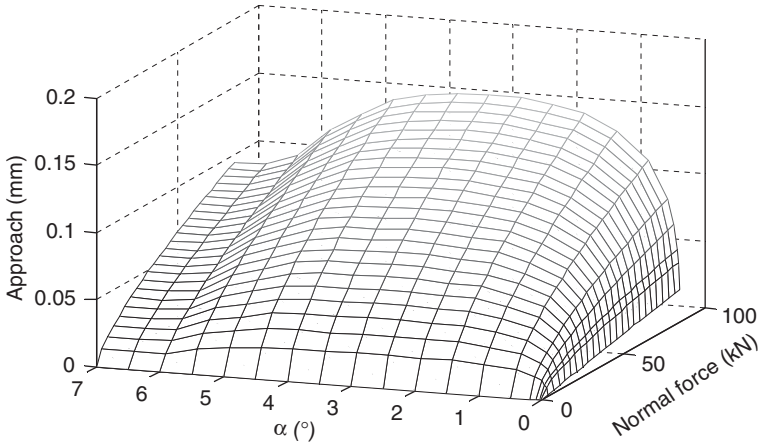


Fig. 6. Approach of centres of the two elastic bodies in contact in relation to the load and the angle of wheel rotation. $\alpha = 0^\circ$ indicates complete contact between fresh flat and rail.

both the elastic contact model and the rigid model with the same data as in the above example. As can be seen, using the elastic contact model, the deviation in the application point of the transmitted force is smoother around $\alpha = 0^\circ$, which can avoid numerical problems when integrating the differential equations.

### 2.5. Railpads

Nonlinear behaviour is mainly associated with the elements interconnecting the subsystems, as in the case of wheel–rail contact dealt with above but also for railpads and ballast.

The stiffness and damping properties of the railpad determine the force $F_{rs}^{p}$ transmitted between rails and sleepers. The force is a function of the relative displacement $\chi$ of the elements which are joined by the railpad, and its time derivative $\dot{\chi}$ according to

$$F_{rs}^{p} = k_p\chi + c_p\dot{\chi} + h_p(\chi, \dot{\chi}), \tag{10}$$

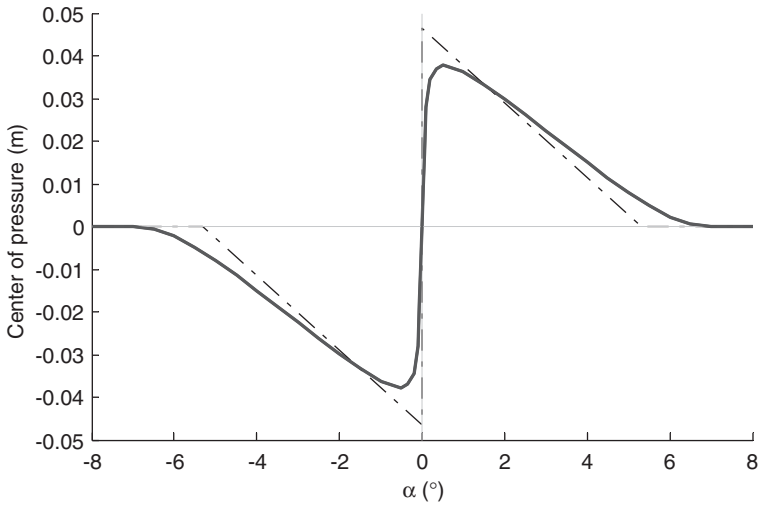


Fig. 7. Longitudinal deviation of the point of application of contact force with respect to the centre position of the axle for a fresh flat considering an elastic (solid) or a non-elastic (dash–dotted) contact model.

where the nonlinearities associated to railpad behaviour are considered in $h_p(\chi, \dot{\chi})$. A similar procedure can be adopted to model the characteristics of the ballast.

## 3. Solving the interaction problem

The time response of the system is obtained by integrating the set of differential equations (4), (6) and (7) by using a numerical Runge–Kutta or Adams type algorithm. The equations are coupled by the terms corresponding to the interaction forces, i.e. the forces transmitted through wheel–rail contacts, railpads and ballast, which depend on relative displacements and velocities as described in the previous section. Displacements in physical coordinates, required to calculate the forces transmitted through railpads and contacts, and the values of the force terms which appear in the differential equations (4) and (6) are obtained through the modal transformations (1) and (2).

As the boundary conditions of the rail model are free–free, the simulation starts in the third sleeper bay in order to obtain a stationary response more quickly. The static displacements are taken as initial conditions in the simulation.

Problem size depends on the number of rails and sleepers, the number of vibration modes considered in the modal descriptions of these elements, and the number of coordinates considered in the vehicle model. It is particularly important in this method to determine the appropriate number of vibration modes to be considered in the modal description of the system, see the next section.

## 4. Modal truncation

### 4.1. Introduction

The proposed method requires a simplification by modal truncation of Eqs. (1) and (2). The truncation of rail modes is the most significant for model accuracy, and it therefore defines the frequency range in which the model is applicable. In order to determine the number of necessary modes, a criterion based on track FRF accuracy is developed using a modal substructuring procedure which applies the same simplifying hypothesis as the proposed method. Using the modal substructuring technique described in the next section, it is possible to obtain the FRF and to verify exact function convergence for a range of frequencies by increasing the number of modes.

### 4.2. Track FRF

The method for obtaining the FRF is based on the assembly of the linearised equations of motion related to the modal coordinates of each substructure (rails and sleepers). Fig. 8 shows the set of coordinates which are considered, corresponding to rail and sleeper displacements at railpad contact points. Vectors $\mathbf{v}_r$ and $\mathbf{u}_s$ define the selected rail $r$ and sleeper $s$ displacements.

Considering the modal transformation defined in Eqs. (1) and (2), the relation between space and modal coordinates considered in the problem can be written as

$$\begin{Bmatrix} \mathbf{v}_1 \\ \mathbf{v}_2 \\ \hdashline \mathbf{u}_1 \\ \vdots \\ \mathbf{u}_{N_s} \end{Bmatrix} = \left[\begin{array}{cc:ccc} \boldsymbol{\Phi} & \mathbf{0} & & \mathbf{0} & \\ \mathbf{0} & \boldsymbol{\Phi} & & & \\ \hdashline & & \boldsymbol{\Psi} & & \mathbf{0} \\ & \mathbf{0} & & \ddots & \\ & & \mathbf{0} & & \boldsymbol{\Psi} \end{array}\right] \begin{Bmatrix} \mathbf{q}_1^R \\ \mathbf{q}_2^R \\ \hdashline \mathbf{q}_1^S \\ \vdots \\ \mathbf{q}_{N_s}^S \end{Bmatrix} \rightarrow \mathbf{x} = \mathbf{T}\mathbf{q}, \tag{11}$$

where the vector $\mathbf{v}_r$ contains the displacements $\{v_{r1} \dots v_{rN_s}\}^{\mathrm{T}}$ of rail $r$ and the vector $\mathbf{u}_s$ includes the displacements of sleeper $s$. Vectors $\mathbf{q}_r^R$ and $\mathbf{q}_s^S$ are the displacements of rail $r$ and sleeper $s$ expressed in modal coordinates.

Linearising railpad characteristics, transmitted forces between rails and sleepers (see Fig. 9) can be calculated by

$$\mathbf{F}_p = -\mathbf{K}_p\mathbf{x} - \mathbf{D}_p\dot{\mathbf{x}}, \tag{12}$$

where matrices $\mathbf{K}_p$ and $\mathbf{D}_p$ are obtained from a linear approximation of Eq. (10). The ballast properties can be included by means of a similar procedure as described above for the railpads, or by calculating the natural

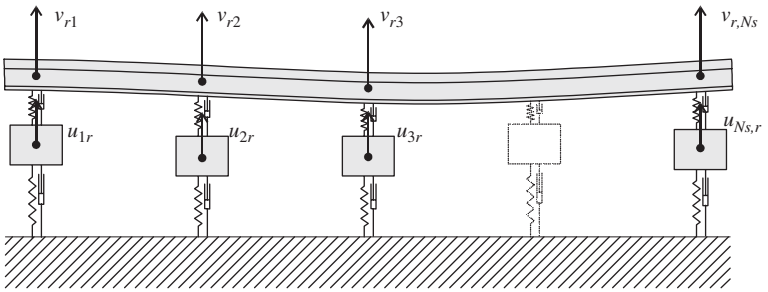


Fig. 8. Displacements considered in the modal substructuring model.

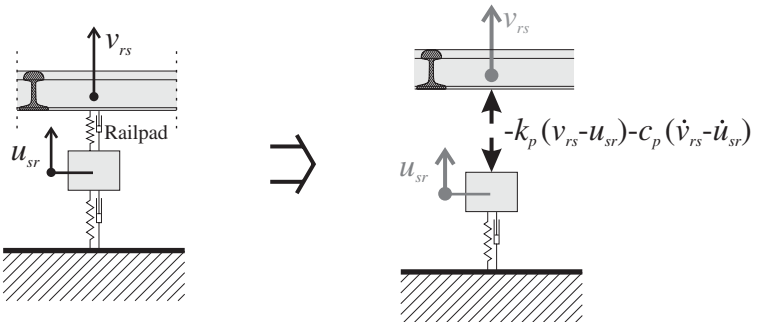


Fig. 9. Railpad forces in the linear model.

frequencies of the sleepers from a Winkler beam model. For the assembled track model, according to Eqs. (3)–(6), the equation of motion in matrix form corresponding to the set of modal coordinates is

$$\ddot{\mathbf{q}} + \mathbf{d}\dot{\mathbf{q}} + \mathbf{k}\mathbf{q} = \mathbf{f}, \tag{13}$$

where $\mathbf{d}$ and $\mathbf{k}$ are diagonal matrices containing the modal damping and modal stiffness properties. The elements of the diagonal in matrix $\mathbf{d}$ are $2\xi_n\omega_n$ for the sleeper coordinates and $2\zeta_m\lambda_m$ for the rail coordinates. The diagonal of matrix $\mathbf{k}$ contains the squares of the natural frequencies of the rails and sleepers. The vector $\mathbf{f}$ expresses the forces transmitted through the railpads (and ballast) and the wheel–rail contact forces in modal coordinates. The transformation which relates the physical and modal forces is

$$\mathbf{f} = \mathbf{T}^{\mathrm{T}}(\mathbf{F}_p + \mathbf{F}_c), \tag{14}$$

where $\mathbf{F}_c$ contains the wheel–rail contact forces. Substituting $\mathbf{f}$ and $\mathbf{x}$ values in Eq. (13) and reordering gives

$$\ddot{\mathbf{q}} + (\mathbf{d} + \mathbf{T}^{\mathrm{T}}\mathbf{D}_p\mathbf{T})\dot{\mathbf{q}} + (\mathbf{k} + \mathbf{T}^{\mathrm{T}}\mathbf{K}_p\mathbf{T})\mathbf{q} = \mathbf{T}^{\mathrm{T}}\mathbf{F}_c, \tag{15}$$

which provides the FRF matrix for modal coordinates $\mathbf{q}$ as

$$\mathbf{H}_q(\omega) = [-\omega^2\mathbf{I} + \mathrm{i}\omega(\mathbf{d} + \mathbf{T}^{\mathrm{T}}\mathbf{D}_p\mathbf{T}) + (\mathbf{k} + \mathbf{T}^{\mathrm{T}}\mathbf{K}_p\mathbf{T})]^{-1}. \tag{16}$$

The FRF for physical coordinates $\mathbf{x}$ is finally calculated as

$$\mathbf{H}_x(\omega) = \mathbf{T}\mathbf{H}_q(\omega)\mathbf{T}^{\mathrm{T}}. \tag{17}$$

In order to obtain the FRF of a point away from the railpad contact, the displacement of this point must be added in the vector $\mathbf{x}$ as a new coordinate.

### 4.3. Model fit by FRF

Fig. 10 shows a set of FRFs (receptance) calculated either by the proposed method or with a FE model. Two results with the proposed model have been calculated using modal properties for the rail obtained from either a Timoshenko or an Euler beam model. A third FRF has been calculated using a FE model where 16 Timoshenko beam elements per sleeper bay have been used in the rail model. The properties of these models correspond to those of the discrete support model in Ref. [3]. A track model with 25 sleeper bays and with free–free boundary conditions at both rail ends is considered. The FRF is studied in one point on the rail at the mid-section of the track model. It is observed that the results obtained from the proposed model using the

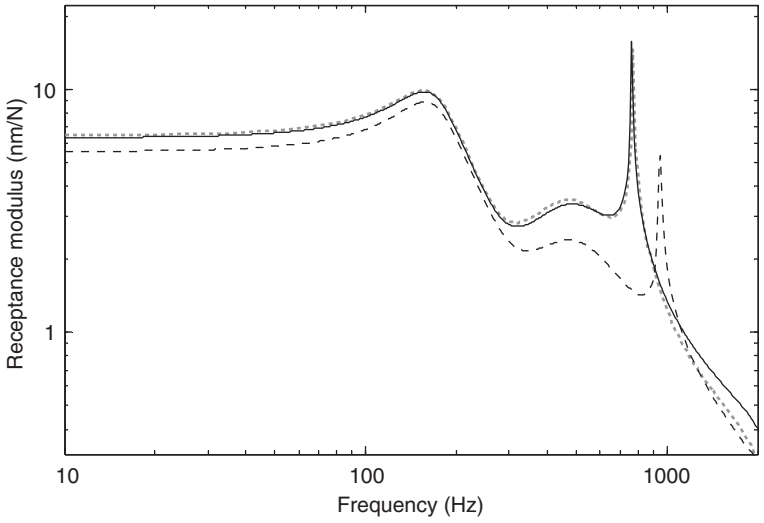


Fig. 10. FRF for a model with 25 sleeper bays. Comparison of results from FE model (dotted) and model based on the suggested substructuring method: modal properties from Euler beam model (dash–dotted) and Timoshenko beam model (solid).

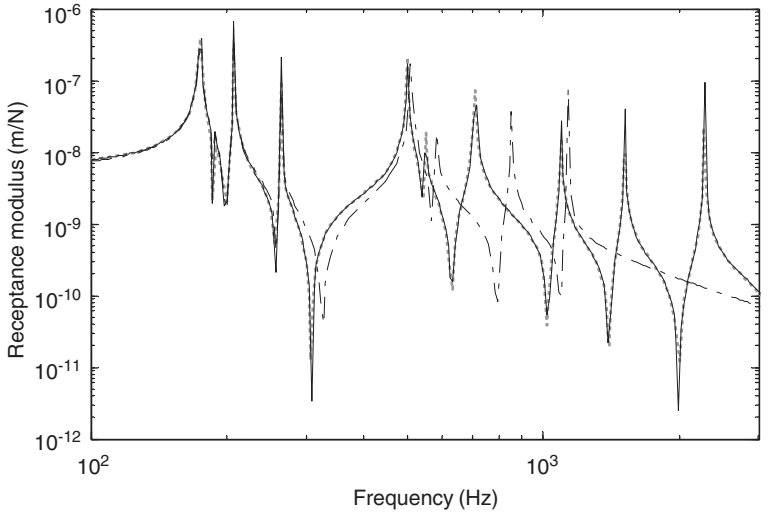


Fig. 11. FRF for a non-damped model with three sleeper bays. Comparison between FE (dotted) results and substructuring method: 4 modes (dash–dotted) and 10 modes (solid).

Timoshenko beam model agrees well with the FRF obtained from the FE model. The proposed model with rail modal properties obtained from an Euler beam model gives similar results to those calculated by Grassie et al. [3]. However, an accurate FRF can only be obtained from the proposed model if a sufficient number of modes in the rail is considered.

The influence of the number of rail modes on the FRF obtained by the proposed model is shown in Fig. 11. The FRF is calculated considering 4 or 10 rail vibration modes, and it is compared with the FRF obtained from a FE model. The track properties are the same as in the previous example. In order to evaluate the influence of all the modes, damping is not considered and the track receptance is calculated at a position on the rail where none of the modes has a zero deflection (this position is located at distance $2^{-0.5}$ times the span length from the sleeper). In this case, a track with only 3 sleeper bays is used so that the FRF is composed of a reduced number of resonances in order to achieve a clearer resolution in the frequency range up to 3 kHz. It is observed that it is possible to fit the FEM results with only 10 rail modes.

By increasing the number of sleeper bays and considering a wider frequency range, more vibration modes must be included in the rail model. The graph in Fig. 12 shows the number of modes required to fit the exact FRF for different frequency ranges and number of sleeper bays. The criterion used for evaluating the accuracy of the estimated FRF $H^*$ with respect to the exact function $H$ in the frequency range $[0, f_{\max}]$ is

$$100\sqrt{\frac{1}{f_{\max}}\int_0^{f_{\max}}\frac{(|H^*|-|H|)^2}{|H|^2}\,\mathrm{d}f}<2\% \tag{18}$$

considering the exact function as that corresponding to a model with 120 rail vibration modes.

## 5. Results

In order to verify the proposed model in the time domain, a benchmark test of a moving wheelset on a track has been performed to compare results to those obtained by a method previously presented by the CHARMEC group in Ref. [19]. The method used as reference has been validated in Ref. [20] and it has been compared in a benchmark test in Ref. [21].

The parameters used in the simulations were selected from Ref. [21]. Table 1 summarises the mechanical properties of track and vehicle. The rail is considered as a Rayleigh–Timoshenko beam and the sleepers are modelled as Euler–Bernoulli beams on a Winkler foundation. Railpads are modelled as springs and viscous dampers in parallel and viscous dampers account for the ballast damping. A total of 51 sleeper bays are

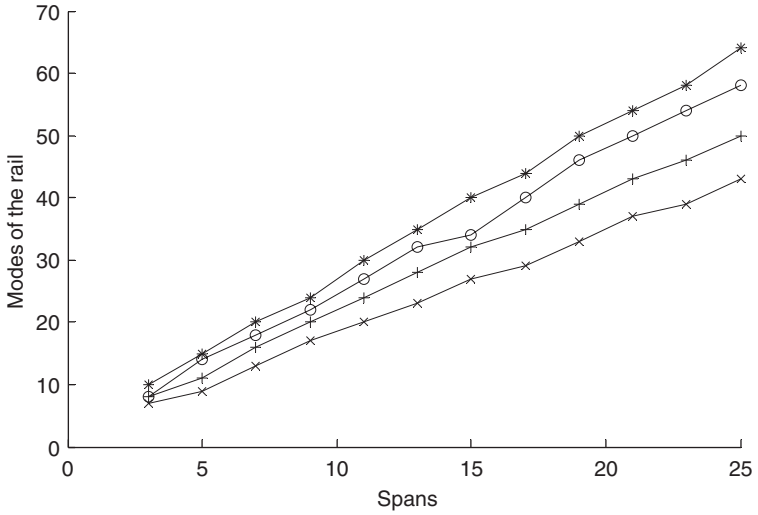


Fig. 12. Number of rail vibration modes which need to be considered in relation to the number of sleeper bays in the track model. Influence of spectrum width: 0–1 kHz ( × ), 0–2 kHz ( + ), 0–3 kHz (○) and 0–4 kHz (*).

Table 1
Input data for vehicle and track models

| Denotation | Parameter | Value |
|---|---|---|
| Track | | |
| $E_r$ | Young's modulus of rail | 210 GN/m$^2$ |
| $\nu_r$ | Poisson's ratio of rail | 0.3 |
| $I_r$ | Rail moment of inertia | $3.05 \times 10^{-5}$ m$^4$ |
| $A_r$ | Rail cross-sectional area | $7.69 \times 10^{-3}$ m$^2$ |
| $k_r$ | Timoshenko shear coefficient | 0.32 |
| $\rho_r$ | Rail density | 7700 kg/m$^3$ |
| $L_r$ | Rail length | 32.5 m |
| $N_s$ | Number of sleepers | 51 |
| $E_s$ | Young's modulus of sleeper | 64 GN/m$^2$ |
| $\nu_s$ | Poisson's ratio of sleeper | 0.15 |
| $I_s$ | Sleeper moment of inertia | $1.75 \times 10^{-4}$ m$^4$ |
| $A_s$ | Sleeper cross-sectional area | $5.138 \times 10^{-2}$ m$^2$ |
| $\rho_s$ | Sleeper density | 3070 kg/m$^3$ |
| $L_s$ | Sleeper length | 2.36 m |
| $D_s$ | Distance between sleepers | 0.65 m |
| $K_p$ | Railpad stiffness | 150 MN/m |
| $C_p$ | Railpad damping | 50 kN s/m |
| $K_b$ | Ballast stiffness per rail seat | 67.8 MN/m$^2$ |
| $C_b$ | Ballast damping per rail seat | 25.4 kN s/m$^2$ |
| Vehicle | | |
| $M_c$ | Carbody mass | 44,800 kg |
| $M_b$ | Bogie frame mass | 4000 kg |
| $I_b$ | Bogie frame pitch moment of inertia | 1600 kg m$^2$ |
| $M_w$ | Wheelset mass | 1800 kg |
| $P_o$ | Wheel–rail static load | 74.6 kN |
| $L_w$ | Distance between wheels in a single bogie | 2.5 m |
| $K_H$ | Constant of Hertzian contact model | 90 GN/m$^{3/2}$ |
| $K_{s1}$ | Primary suspension stiffness | 1 MN/m |
| $C_{s1}$ | Primary suspension damping | 10 kN s/m |
| $K_{s2}$ | Secondary suspension stiffness | 1.4 MN/m |
| $C_{s2}$ | Secondary suspension damping | 40 kN s/m |

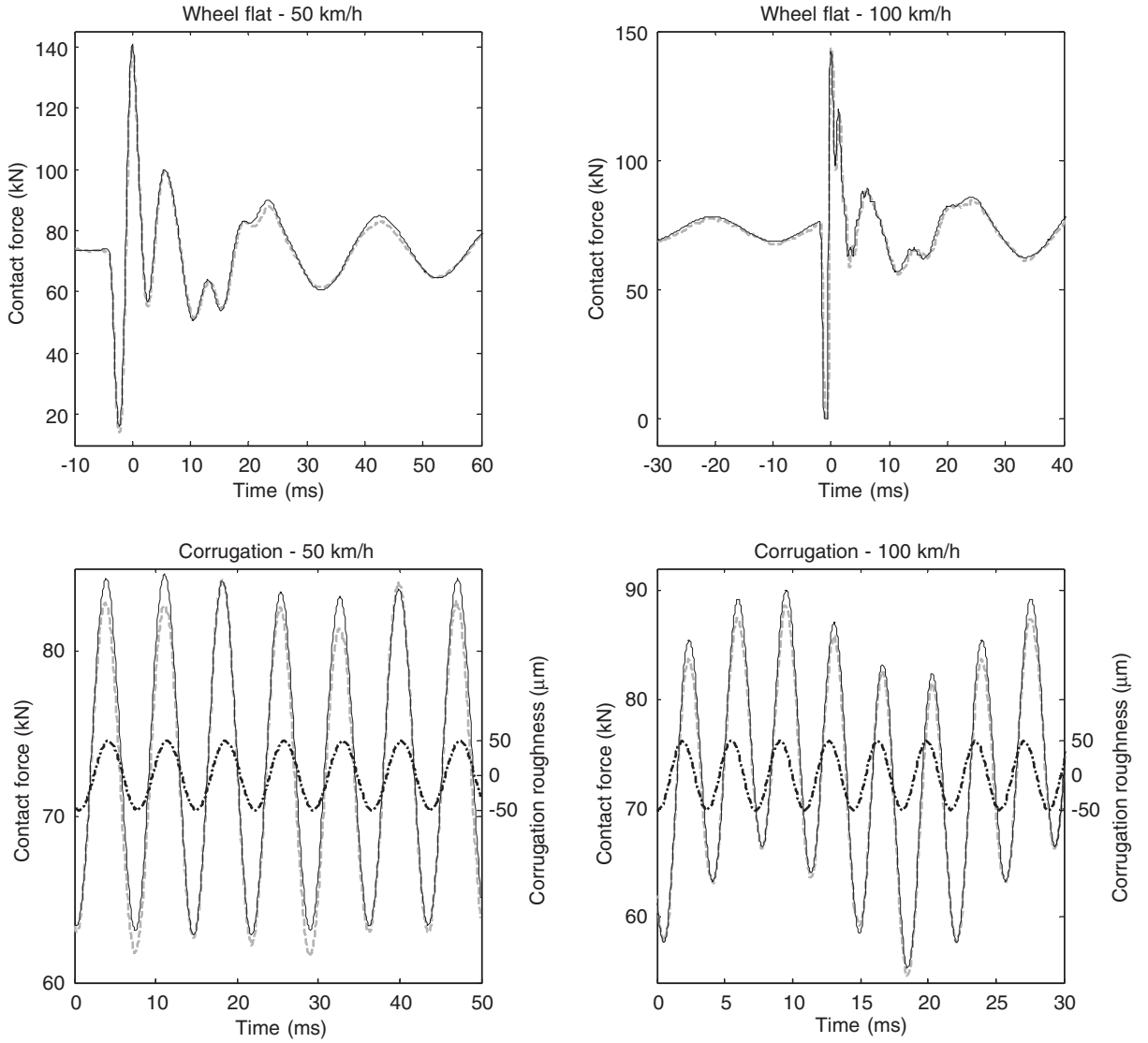


Fig. 13. Comparison of results from the proposed model (solid) and the model developed by CHARMEC (dashed). The calculations correspond to dynamic responses due to a wheelflat or rail corrugation (the corrugation irregularity is shown as the dash–dotted line).

considered to represent the track, and 90 modes are used for each rail. The selected load cases study the dynamic responses due to a rounded wheel flat or a corrugated rail.

Results are illustrated in Fig. 13. In these figures, the wheel–rail contact force responses are illustrated for some combinations of irregularity and train speed. Good agreement between the results from the two models is observed.

## 6. Conclusions

This work presents a method for simulation of the dynamic interaction between train and track. The method is computationally efficient in the sense that a reduced number of coordinates is sufficient. The method proposes a modal substructuring approach of the system by modelling those elements with linear dynamic behaviour (rails and sleepers) with modal coordinates, and by introducing interconnection elements between these structures (wheel–rail contact, railpads and ballast) by means of their interaction forces. The

technique offers the possibility of including complex models of inter-structural elements such as non-Hertzian wheel–rail contact, and nonlinear properties of ballast and rail pads.

The method has been tested against a validated method developed by CHARMEC. Good agreement was obtained for the simulated dynamics caused by a wheelflat or by rail corrugation when linear models of vehicle and track were considered.

## Acknowledgements

The authors would like to thank *Generalitat Valenciana* and *Vicerrectorado de Investigación, Desarrollo e Innovación* (*UPV*) for their support of the research project. They also owe much gratitude to all the members of *CHARMEC* at *Chalmers University of Technology* in Gothenburg, Sweden.

## References

[1] K.L. Knothe, S.L. Grassie, Modelling of railway track and vehicle/track interaction at high frequencies, *Vehicle System Dynamics* 22 (1993) 209–262.
[2] K. Popp, H. Kruse, I. Kaiser, Vehicle–track dynamics in the mid-frequency range, *Vehicle System Dynamics* 31 (1999) 423–464.
[3] S.L. Grassie, R.W. Gregory, D. Harrison, K.L. Johnson, The dynamic response of railway track to high frequency vertical excitation, *Proceedings of the Institution of Mechanical Engineers, Part C: Journal of Mechanical Engineering Science* 24 (2) (1982) 77–90.
[4] S.P. Patil, Response of infinite railroad track to vibrating mass, *Journal of Engineering Mechanics* 114 (4) (1988) 688–703.
[5] D.G. Duffy, The response of an infinite railroad track to a moving, vibrating mass, *Journal of Applied Mechanics* 57 (1990) 66–73.
[6] C. Andersson, Modelling and Simulation of Train–Track Interaction Including Wear. Ph.D. Thesis, Department of Applied Mechanics, Chalmers University of Technology, Göteborg, 2003.
[7] R.V. Dukkipatti, R. Dong, Idealized steady state interaction between railway vehicle and track, *Proceedings of the Institution of Mechanical Engineers, Part F: Journal of Rail and Rapid Transit* 213 (1) (1999) 15–29.
[8] J.C.O. Nielsen, A. Igeland, Vertical dynamic interaction between train and track—influence of wheel and track imperfections, *Journal of Sound and Vibration* 187 (5) (1995) 825–839.
[9] J.C.O. Nielsen, J. Oscarsson, Simulation of dynamic train−track interaction with state-dependent track properties, *Journal of Sound and Vibration* 275 (2004) 515–532.
[10] T.X. Wu, D.J. Thompson, A hybrid model for the noise generation due to railway wheel flats, *Journal of Sound and Vibration* 251 (1) (2002) 115–139.
[11] C. Andersson, T. Abrahamsson, Simulation of interaction between a train in general motion and a track, *Vehicle System Dynamics* 38 (2002) 433–455.
[12] W. Weaver, S.P. Timoshenko, D.H. Young, *Vibration Problems in Engineering*, Willey, New York, 1990.
[13] S.H. Farchaly, M.G. Sheb, Exact frequency and mode shape formulae for studying vibration and stability of Timoshenko beam system, *Journal of Sound and Vibration* 180 (2) (1995) 205–227.
[14] S.G. Newton, R.A. Clark, An investigation into the dynamic effects on the track of wheelflats on railway vehicles, *Proceedings of the Institution of Mechanical Engineers, Part C: Journal of Mechanical Engineering Science* 21 (4) (1979) 287–297.
[15] J.M. Tunna, Wheel/rail forces due to wheel irregularities, in: Proceedings of the Ninth International Wheelset Congress, Montreal, Canada, 1988 (paper 6-2).
[16] K.L. Johnson, *Contact Mechanics*, Cambridge University Press, Cambridge, 1985.
[17] D.A. Hills, D. Nowell, *Mechanics of Fretting Fatigue*, Kluwer Academic Publishers, Dordrecht, 1994.
[18] J.J. Kalker, *Three-Dimensional Elastic Bodies in Rolling Contact*, Kluwer Academic Publishers, Dordrecht, 1990.
[19] J.C.O. Nielsen, T.J.S. Abrahamsson, Coupling of physical and modal components for analysis of moving non-linear dynamic systems on general beam structures, *International Journal for Numerical Methods in Engineering* 33 (1992) 1843–1859.
[20] A. Johansson, J.C.O. Nielsen, Out-of-round railway wheels—wheel–rail contact forces and track response derived from field tests and numerical simulations, *Proceedings of the Institution of Mechanical Engineers, Part F: Journal of Rail and Rapid Transit* 217 (2003) 135–146.
[21] S.L. Grassie, Benchmark test for models of railway track and of vehicle/track interaction at relatively high frequencies, *Supplement to Vehicle System Dynamics* 24 (1995) 355–362.